DOI: 10.1093/brain/awh276 *Brain* (2004), **127,** 2551–2557

Mapping of the SCA23 locus involved in autosomal dominant cerebellar ataxia to chromosome region 20p13-12.3

D. S. Verbeek,[3] B. P. van de Warrenburg,[1] P. Wesseling,[2] P. L. Pearson,[3] H. P. Kremer[1] and R. J. Sinke[3]

Departments of [1]Neurology and [2]Pathology, University Medical Center, Nijmegen, and [3]Department of Biomedical Genetics, University Medical Center, Utrecht, the Netherlands

Correspondence to: Dineke Verbeek, Department of Biomedical Genetics, Stratenum 2.112, University Medical Center Utrecht, Universiteitsweg 100, 3584 CG, the Netherlands
E-mail: D.S.Verbeek@med.uu.nl

Summary

We report upon a Dutch autosomal dominant cerebellar ataxia (ADCA) family, clinically characterized by a late-onset (>40 years), slowly progressive, isolated spinocerebellar ataxia (SCA). Neuropathological examination in one affected subject showed neuronal loss in the Purkinje cell layer, dentate nuclei and inferior olives, thinning of cerebellopontine tracts, demyelination of posterior and lateral columns in the spinal cord, as well as ubiquitin-positive intranuclear inclusions in nigral neurons that were considered to be Marinesco bodies. Data obtained from the genome-wide linkage analysis revealed a maximal lod score of 3.46 at θ = 0.00 for marker D20S199. This new SCA locus, on chromosome region 20p13-p12.3, was designated SCA23 after approval by the HUGO Nomenclature Committee. Currently, candidate genes are being screened for mutations within the SCA23 interval. In addition to the recently identified SCA14, SCA19 and FGF14 families, SCA23 is yet another novel SCA locus in the Dutch ADCA population, which further defines the genetic heterogeneity of ADCA families in the Netherlands.

Keywords: autosomal dominant cerebellar ataxia; neurodegenerative disorder; polyglutamine; human genetics; linkage analysis

Abbreviations: ADCA = autosomal dominant cerebellar ataxia; FGF14 = fibroblast growth factor 14; lod = logarithm of odds; SCA = spinocerebellar ataxia

Received April 20, 2004. Revised June 18, 2004. Accepted June 22, 2004. Advanced Access publication August 11, 2004

Introduction

The autosomal dominant cerebellar ataxias (ADCAs) are a group of seriously invalidating disorders characterized by gait and limb ataxia, disturbances of speech and oculomotor control, in combination with variable other clinical features and usually with an adult age at onset (Harding, 1983). Harding's classification of ADCAs into type I–III, based on the differential clinical features, is gradually being substituted by a classification based on molecular-genetic characteristics.

Since 1993, 11 spinocerebellar ataxia (SCA) genes have been cloned (SCA 1–3, 6–8, 10, 12, 14, 17 and fibroblast growth factor-14 (*FGF14*)) and an additional 12 SCA loci (SCA 4, 5, 11, 13, 15, 16, 18- 21, 24 and 25) have been identified (HUGO Nomenclature Committee: http://www.gene.ucl.ac.uk/cgi-bin/nomenclature/searchgenes.pl) (Orr *et al*., 1993; Kawaguchi *et al*., 1994; Ranum *et al*., 1994; David *et al*., 1996; Flanigan *et al*., 1996; Imbert *et al*., 1996; Pulst *et al*., 1996; Sanpei *et al*., 1996; Zhuchenko *et al*., 1997; Holmes *et al*., 1999; Koide *et al*., 1999; Koob *et al*., 1999; Matsuura *et al*., 1999; Worth *et al*., 1999; Zu *et al*., 1999; Herman-Bert *et al*., 2000; Yamashita *et al*., 2000; Devos *et al*., 2001; Miyoshi *et al*., 2001; Nakamura *et al*., 2001; Swartz *et al*., 2002; Verbeek *et al*., 2002; Chen *et al*., 2003; Knight *et al*., 2003, 2004; Stevanin *et al*., 2004).

In SCA 1–3, 6, 7, and 17, the mutational mechanism is known to be a repeat expansion of coding CAG stretches leading to elongated polyglutamine tracts in the otherwise unrelated encoded proteins. However, in the SCA 8, 10, and 12 genes, the mutation involves a non-coding CTG, ATTCT and CAG repeat expansion, respectively (Holmes *et al*., 1999; Koob *et al*., 1999; Matsuura *et al*., 2000). Interestingly, the most recently identified mutations in the *FGF14* gene and the SCA14 (*PRKC6*) gene turned out to be missense

mutations (Yue *et al*., 1997; Chen *et al*., 2003; van de Warrenburg *et al*., 2003; van Swieten *et al*., 2003; Yabe *et al*., 2003). Based on results of diagnostic testing of ADCA families, the estimated prevalence of ADCA in the Netherlands is about three per 100 000 individuals (van de Warrenburg *et al*., 2002). In ~30% of the Dutch ADCA families, no repeat expansion is identified in the SCA 1–3, 6, and 7 genes. So far, the SCA 10, 12 or 17 repeat expansions have not been reported in the Netherlands and the contribution of *FGF14* mutations remains to be established. In addition, the contribution of the SCA14 mutations is currently being explored in our laboratory. So far, the SCA14 mutations seem to be restricted to the Cys2 region of the C1 domain, indicating a particular role for this part of the gene or the mutations that were identified. Still, we hypothesize that yet unidentified SCA genes are present in Dutch ADCA families.

Here, we present a Dutch ADCA family, clinically characterized by a late-onset (>40 years), slowly progressive, isolated SCA. Linkage analysis localized the disease gene to chromosome region 20p13-p12.3, and this locus was designated SCA23 (approved by the HUGO Nomenclature Committee). The identification of SCA23 further adds to the genetic heterogeneity of Dutch ADCA families.

Methods

The patients

The pedigree of the three-generation family that participated in this study is shown in Fig. 1. In order to maintain confidentiality, some individuals are depicted with the symbol sex unknown. All participating family members signed an informed consent. The study was approved by the University Medical Center Utrecht (Utrecht) Medical Ethical Committee. DNA samples were available from nine affected individuals and five presumptive unaffected relatives. Five of the affected family members were subjected to a thorough neurological examination. One asymptomatic carrier was detected.

Neuropathology and immunohistochemistry

The brain of subject II:11, who died in 1996 at the age of 80 years, was available for neuropathological examination and immunohistochemical studies. After formalin fixation and external neuropathological examination, the brain and spinal cord were examined at the cut surface, and multiple samples were taken and embedded in paraffin for histology. The following tinctorial stainings were performed on 4 mm histological sections of these samples: haematoxylin and eosin (H&E), Bodian silver, and a combined luxol fast blue (LFB) and H&E (LFB–H&E) staining. In addition, on sections of relevant areas (brain stem, spinal cord, cerebellum, hippocampus)

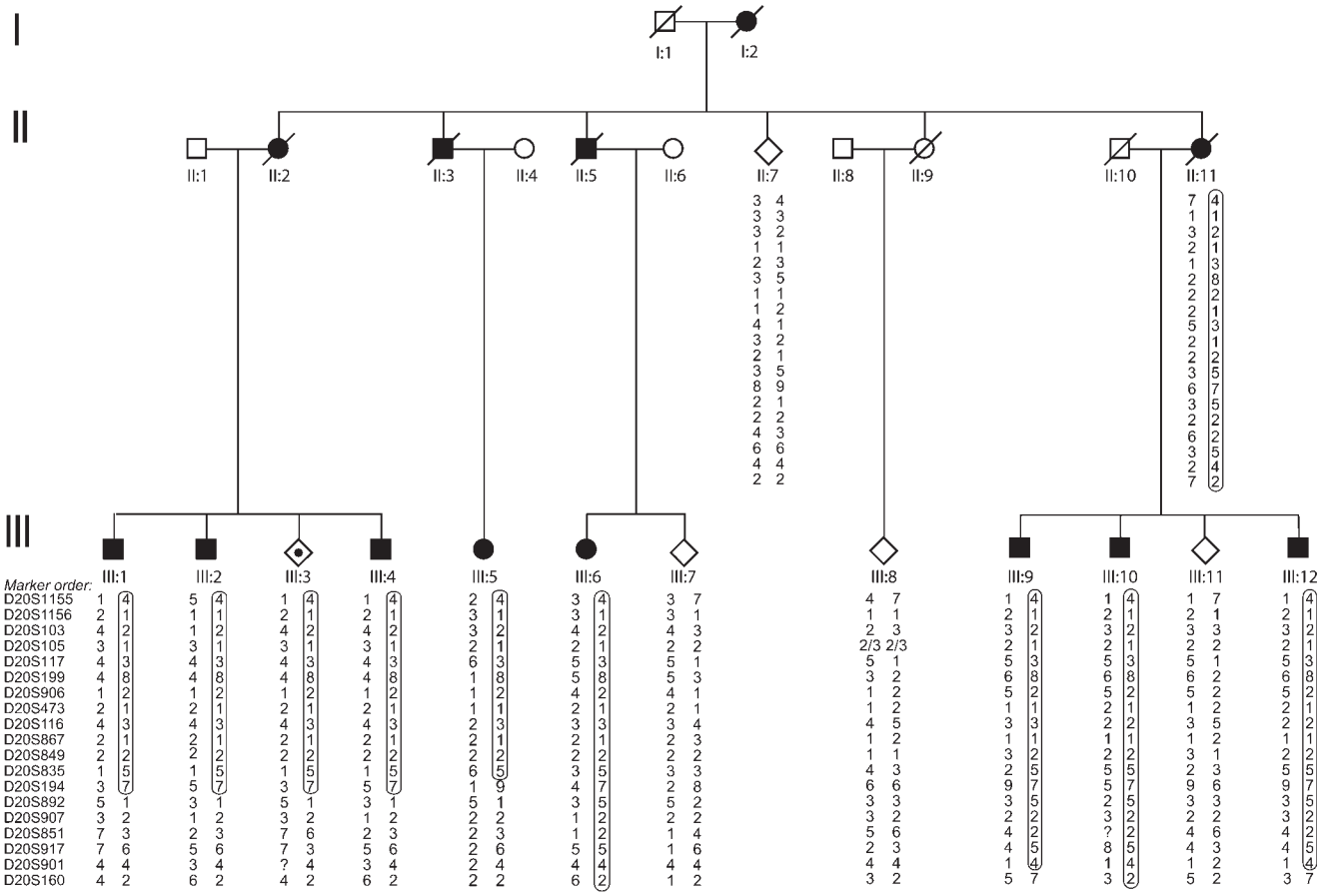

Fig. 1 Pedigree of the SCA23 family. Haplotype analysis is shown for 19 chromosome 20 markers. To maintain confidentiality, some individuals are depicted with the symbol sex unknown. The disease haplotype is boxed. Open figures = unaffected; closed figures = affected; dotted figures = asymptomatic carrier; square = male; circle = female; diamond = unknown sex; / = deceased.

immunohistochemical stainings were performed for ubiquitin (DAKO Cytomation, Heverlee, Belgium), tau (Innogenetics, Gent, Belgium), β-amyloid (DAKO Cytomation), α-synuclein (Neomarkers/Labvision, Fremont CA, USA), 1C2 (Chemicon International, Temecula, CA, USA), and ataxin-3 (Paulson *et al*., 1997).

Mutation analysis of known SCA genes

High molecular weight genomic DNA was isolated from peripheral blood leukocytes using routine salting-out procedures. Direct mutational analysis of trinucleotide repeat expansions of the SCA 1–3, 6–8, 12 and 17 genes was performed, but no repeat expansions were observed (data not shown). The other SCA loci (SCA 4–6, 10, 11, 13, 14, 16 and 19) were excluded by two-point linkage analysis (lod score < −2.0). The polymorphic markers used were selected from the Marshfield database: http://research.marshfieldclinic.org/genetics/Map_Markers/maps/IndexMapFrames.html.

Genome-wide genotyping analysis

After excluding the known SCA loci as candidates, a genome-wide scan was performed. The screening set consisted of 350 polymorphic markers, covering the whole genome. The average spacing between two adjacent markers was 10–15 cM. The protocol used to amplify the polymorphic markers was as described previously (Verbeek *et al*., 2002). Multiplex PCR products with HEX and FAM or HEX and TET labels were pooled. Finally, 1 ml of these pools were mixed with 4 ml HiDi^{tm} (highly deionized formamide) including the internal lane standard ROX (Applied Biosystems, Foster City, CA, USA), and run on an automated high-throughput capillary electrophoresis ABI3700 machine (Applied Biosystems). Subsequently, fragment analysis and genotyping were performed using Genescan (v3.5 NT) and Genotyper (v2.1) software (Applied Biosystems). Two raters scored all genotypes independently.

Linkage analysis

Two-point lod (logarithm of odds) scores were calculated for each marker with the program MLINK (Lathrop and Lalouel, 1984) of the software package FASTLINK (v5.2) (Lathrop and Lalouel, 1984), using an affected-only strategy assuming an autosomal dominant mode of inheritance, a disease frequency of 1:100 000, and equal allele frequencies of the markers. Two-point lod scores >1.0 were considered to indicate regions of interest. These genomic regions were further fine mapped by testing additional markers and haplotype analysis. With the program LINKMAP of the LINKAGE (v5.2) package (Lathrop and Lalouel, 1984), a multi-point analysis was performed to confirm the size of the candidate region.

Results

Clinical characteristics

In the five family members examined, the age at onset ranged from 43 to 56 years (mean 50.4 ± 4.9 years) and disease duration varied from 1 to 23 years (mean 10.2 ± 8.4 years) (Table 1). The presence of clinical anticipation could not be studied because we were only able to examine affected subjects from the second generation. The age at onset of individual II:11, of whom blood and brain tissue was preserved, could not be extracted accurately from clinical records. Gait difficulties were the presenting feature in three subjects, while cycling difficulties and a simultaneous deterioration of gait and speech were the presenting signs in two others. After onset of disease, all displayed a slowly progressive, isolated SCA. In addition to gait and/or limb ataxia, which were present in all subjects, the neurological examination revealed dysarthria in three, slowing of both saccades and ocular dysmetria in three, decreased vibration sense below the knees in three, hyperreflexia in four, and Babinski's sign in two affected subjects. Clinical severity grossly correlated with the duration of the disease; subject III:4, with a disease duration of 23 years, was wheelchair-bound outdoors. Cognitive deterioration or mental retardation, epilepsy, extrapyramidal features, signs of peripheral nerve involvement or sphincter abnormalities were not present. Neurophysiological studies were not conducted. An MRI-scan of the brain in subject III:4 at the age of 60 years showed severe cerebellar atrophy, normal brain stem structures and basal ganglia, no cerebral cortical atrophy, and multiple small subcortical white matter lesions in the cerebral hemispheres that resembled vascular disease.

Neuropathology

The brain weight was 930 g (normal for age = 1100–1400 g). Macroscopically, the cerebrum, cerebellum, brain stem and

Table 1 *Clinical characteristics of affected family members*

Patient	Sex	Age (years)	Age at onset (years)	Disease duration (years)	Presenting symptom	Gait ataxia	Limb ataxia	Dysarthria	Saccade slowing	Ocular dysmetria	Disturbed distal vibration and position sense	Tendon reflexes	Babinski's sign
III:6	F	62	53	9	G	++	++	−	+	−	++	↑	−
III:1	M	61	56	5	G/S	+	+	+	+	+	++	↑	+
III:2	M	64	51	13	G	+	+	+	−	−	−	N	−
III:4	M	66	43	23	G	+++	+++	+++	+	+	++	↑	+
III:12	M	50	49	1	C	−	±	−	−	±	−	↑	−

M = male; F = female; G = gait difficulties; C = cycling difficulties; S = speech difficulties; − = absent; ± = subtle; + = present or mild; ++ = moderate; +++ = severe; ↑ = increased; N = normal.

spinal cord showed generalized, moderate to severe atrophy. The atrophy was most pronounced in the frontotemporal region of the cerebrum, the vermis of the cerebellum, the basis pontis and the spinal cord. On the cut surface, marked dilatation of the cerebral ventricles was found with moderate, generalized atrophy of the central nuclei. The substantia nigra and locus ceruleus showed normal pigmentation.

Microscopically, pronounced neuronal loss was present in the Purkinje cell layer, especially in the vermis (Fig. 2A and B) and in dentate nuclei and inferior olives, accompanied by variable gliosis and myelin loss in the surrounding white matter. In the basis pontis, both the longitudinal and transverse white matter tracts were well myelinated, but the latter (i.e. cerebellopontine) tracts were relatively small.

No neuronal loss was observed within the pontine nuclei. The substantia nigra and locus ceruleus contained an ample number of pigmented neurons with sparse loose neuromelanin pigment and an occasional Lewy body in the substantia nigra. In the spinal cord, especially in the posterior and lateral columns moderate, dispersed loss of (staining for) myelin was found without inflammatory infiltrate or gliosis; there was no clear loss of motoneurons.

On thorough microscopic examination, only a few neurons in the substantia nigra contained striking intranuclear inclusions (Fig. 2C). These inclusions were round, 2–5 mm in diameter, strongly ubiquitin positive, but negative to the other immunohistochemical stainings (including 1C2 and ataxin-3) and therefore interpreted as Marinesco bodies. No other ubiquitin positive inclusions were found. In the α-synuclein staining, no cortical Lewy bodies were found. In the Bodian silver staining and in the immunohistochemical stainings for tau and β-amyloid, other 'neurodegenerative depositions' were generally scarce (neurofibrillary tangles, neuritic plaques) or absent (amyloid angiopathy, Pick bodies, oligodendroglial inclusions). In the tau-staining, some micro- and astroglial cells in and around central nuclei, dentate nuclei and substantia nigra were positive.

Vascular damage was present in the form of moderate to severe atherosclerosis of the circle of Willis and its major branches, with large recent ischemic necrotic areas in the left insular region (maximum 8 cm; territory of the left medial cerebral artery) and left occipital lobe (maximum 5 cm; territory of left posterior cerebral artery), and dispersed old ischemic necrotic lesions (cerebral white matter, hypothalamus, cerebellar cortex and white matter, basis pontis; maximum 1 cm). General autopsy revealed severe cachexia, emphysema, contractures of especially the lower limbs, and severe atherosclerosis of the large and middle-sized arteries with dispersed old infarcts in kidneys and spleen, myocardial hypertrophy and atheromatous plaques in the pulmonary artery (the latter indicating pulmonary hypertension).

Linkage analysis

The SCA loci were excluded in the initial analysis with two-point lod scores (data not shown). Next, a genome-wide screen was performed and only two genomic regions showed two-point lod scores of >1.0, including regions on

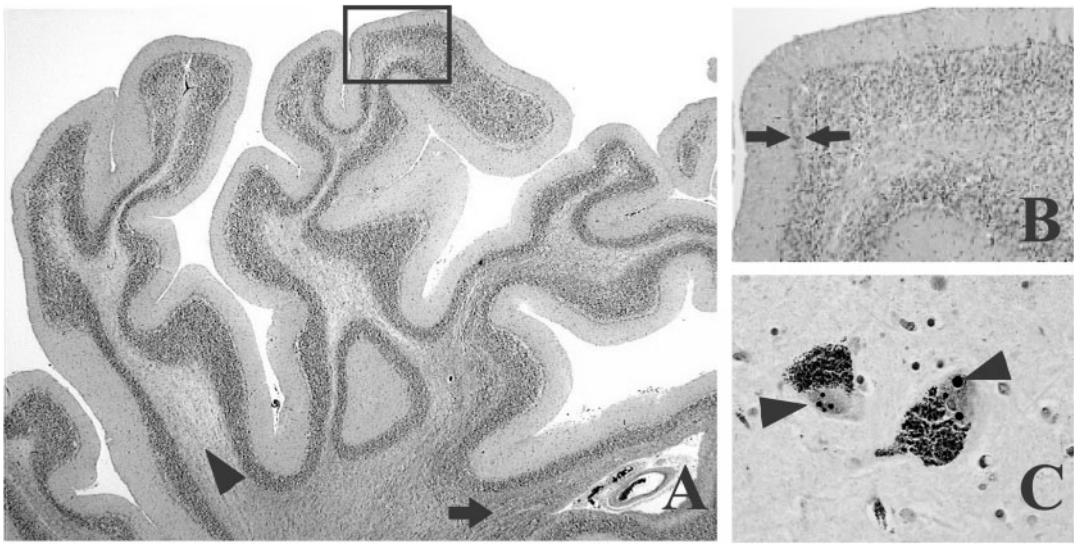

Fig. 2 Neuropathological findings. The cerebellar folia, especially of the rostral vermis (**A**,**B**), show severe atrophy with (sub)total loss of myelin in some parts (lighter staining, loosely textured area of white matter, indicated by arrowhead in **A**) and relative preservation of myelin in other parts of the white matter (darker staining for myelin in more compact area, indicated by arrow in **A**). Panel (**B**) represents a higher magnification of the area indicated by the rectangle in (**A**); it illustrates severe Purkinje cell loss, accompanied by Bergmann gliosis in the affected cerebellar cortex (arrows). Occasional neurons in the substantia nigra contain up to four round, intranuclear inclusions in (arrowheads in **C**, maximum diameter = 5 mm). These are strongly ubiquitin positive, but negative in the 1C2 and ataxin-3 staining and were therefore interpreted as Marinesco bodies. No pathological neuronal intranuclear inclusions were encountered in the CNS of this patient. (**A**,**B**) Luxol fast blue and haematoxylin and eosin staining. (**C**) Ubiquitin staining. Original magnification ×12.5 (**A**), ×100 (**B**) and ×400 (**C**).

Table 2 *Two-point lod scores between the disease locus and 11 chromosome 20*

Markers	Lod score at recombination rate (θ)						
	0.00	0.10	0.20	0.30	0.40	*Zmax*	θ=
D20S1155	2.22	1.82	1.36	0.84	0.3	2.22	0.00
D20S103	1.48	1.19	0.85	0.49	0.15	1.48	0.00
D20S117	2.49	2.06	1.56	0.99	0.38	2.49	0.00
D20S199	3.46	2.82	2.1	1.32	0.5	3.46	0.00
D20S473	0.39	0.34	0.25	0.14	0.04	0.39	0.00
D20S867	1.66	1.2	0.75	0.36	0.09	1.66	0.00
D20S835	2.02	1.68	1.25	0.76	0.27	2.02	0.00
D20S194	−4.57	0.53	0.46	0.26	0.07	0.53	0.10
D20S907	−0.08	−0.04	−0.02	−0.01	−0.01	−0.01	0.30
D20S901	1.27	1.08	0.8	0.48	0.16	1.27	0.00
D20S160	−6.50	−1.01	−0.45	−0.17	−0.04	−0.04	0.40

chromosomes 20 and 22. In addition, analysis of our data might be hampered by the presence of possible asymptomatic mutation carriers, an affected-only strategy was performed. This resulted in a maximal lod score (Z_{max}) of 3.46 at θ = 0.00 for marker D20S199 (Table 2). The order and distance between the markers are based on the Marshfield database from April 2002 (http://research.marshfieldclinic.org/genetics/).

Haplotype and multi-point linkage analysis

Haplotypes were constructed by minimizing the number of possible recombination events (Fig. 1). The candidate interval directly starts from the tip of the short arm of chromosome 20, because no recombination events were detected with the most proximal marker D20S1155. A recombination event was observed in affected individual III:5 with marker D20S194 located at 18.2 cM, which determined the lower boundary of the interval. Multi-point linkage analysis (Fig. 3) based on the affected-only strategy was performed and resulted in a Z_{max} of 3.56. Due to computer restraints, the multi-point analysis was calculated with three markers at the same time. The overlapping parts of the interval showed identical values, indicating that the analysis was performed correctly. The 95% candidate interval (maximum lod = −1) from the multi-point analysis is flanked by marker D20S1155 and marker D20S835, and spans around 15 cM.

Candidate gene analysis

The SCA23 interval is located between the tip of the short arm of chromosome 20 and D20S194, and is ∼18.2 cM in size, corresponding to ∼6.1 Mb, and contains around 100 genes. Our first attempt focused on candidate genes that contain coding triplet repeats. This resulted in the identification of two coding $(CTG)_{5/6}$ stretches in the GFR receptor α-4 (*GFRA4*) gene and the Attractin with dipeptidylpeptidase IV activity (*ATRN*) gene.

Only one coding CAG repeat was identified; this was located in the ubiquitin-conjugating enzyme 7 interacting protein 3 gene. Four other non-coding intronic CAG repeats were located within the boundaries of the genes including β-neoendorphin-dynorphin precursor [*PDYN*; $(CTG)_7$], KIAA1442 protein [*Q9P2A6*; $(CTG)_5$], ring finger protein 24 [*RNF24*; $(CTG)_5$], FK506 binding protein peptidyl prolyl cis trans isomerase [*FKBP1A*; $(CAG)_7$] and signal-regulatory protein β-1 precursor [*SIRP-β-1*; $(CAG)_6$]. Four other CAG and CTG repeats with a maximal length of five repeats were identified, but it remained unclear whether these repeats are coding or non-coding sequences. However, no repeat expansions for any of these genes were observed (data not shown).

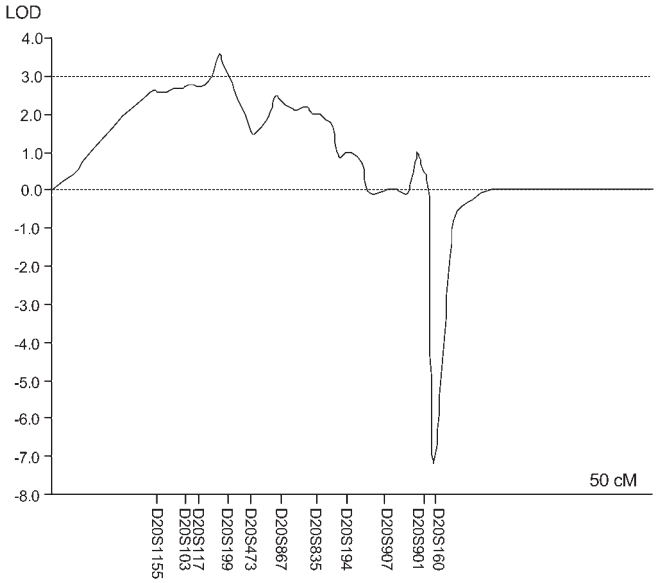

Fig. 3 Multi-point analysis with eleven chromosome 20 markers.

Secondly, only three other genes were selected for missense mutation screening including neuronal cell death inducible kinase (*SKIP3*), major prion protein precursor (*PRNP*) and the prion gene complex downstream (*PRND*). In addition, over-expression of Doppel (*Dpl*), the paralog of the mammalian prion protein (*PrP*), is correlated with ataxia and death of cerebellar neurons in mice. All three genes were excluded as candidates based on our sequence data results.

Discussion

The genome scan in this three-generation Dutch ADCA family resulted in the identification of a novel SCA locus, designated SCA23, on chromosome region 20p13-p12.3. Clinically, the affected family members displayed a late-onset (>40 years), slowly progressive, isolated SCA. Features mainly included gait and limb ataxia, disturbance of oculomotor control, dysarthria and hyperreflexia. As distinctive extracerebellar disease features are absent, the SCA23 phenotype is clinically indistinguishable from other SCA subtypes; relatively pure cerebellar syndromes have also been described in SCA5, SCA6, SCA11, SCA14, SCA15, SCA16 and SCA22 (Schols *et al*., 2004). Genome-wide linkage analysis revealed a maximal two-point lod score (Z_{max}) of 3.46 at $\theta = 0.00$ with marker D20S199. The SCA23 interval is located between the tip of the short arm of chromosome 20 and D20S194, and is ~18.2 cM in size, corresponding to ~6.1 Mb, and containing ~100 genes.

Our candidate genes analysis was unable to identify the SCA23 disease-causing mutation. We focused on candidate genes that contain coding triplet repeats, since this is the most common mutation in the ADCAs worldwide. We also searched for missense mutations in genes that correlated with ataxia and death of cerebellar neurons in mice, considering the fact that the two most recently identified SCA mutations were point mutations.

The neuropathological findings in subject II:11 grossly correspond to previous observations in this group of disorders, although we did not observe the neuronal intranuclear inclusions typically encountered in polyQ-associated ADCAs (Robitaille *et al*., 1997; Schols *et al*., 2004) Some nigral neurons were found to contain ubiquitin-positive intranuclear inclusions, very much reminiscent of Marinesco bodies. In addition, Lewy bodies were occasionally present in nigral neurons. Substantia nigra involvement has been reported in SCA2 and SCA3 patients (Orozco *et al*., 1989; Durr *et al*., 1996). Unfortunately, it is not known whether subject II:11 displayed additional parkinsonian features. Marinesco bodies are non-specific ubiquinated intranuclear inclusions in nigral neurons observed in, for example, normal ageing and Alzheimer's disease. Interestingly, wild-type ataxin-3, the mutated protein in SCA3, was recently found to be recruited to Marinesco bodies in both non-human primates and in myotonic dystrophy patients (Kettner *et al*., 2002; Kumada *et al*., 2002). In our case, we did not find the Marinesco bodies to be immunopositive for ataxin-3, but this may be due to the fact that different antibodies were used. How this finding of Marinesco bodies relates to the pathogenic processes involved in SCA23 and whether this also indicates failure of protein homeostasis mechanisms remains to be established (mainly by identifying the mutated gene product).

In conclusion, the SCA23 locus is a novel locus identified in the Dutch ADCA population. The candidate interval is located on chromosome region 20p13-12.3 and is ~18.2 cM. In an attempt to refine the size of the candidate interval, we are currently trying to identify additional ADCA families that also link to the SCA23 locus.

Acknowledgements

The authors wish to thank all the family members for participating in this study, Jackie Senior for improving the manuscript, and Lude Franke for designing the repeat finder program. We also wish to thank Rob de Vos (Department of Pathology, Medisch Spectrum Twente, the Netherlands) for his help with the immunohistochemical stainings and for fruitful discussions. This work was supported by grant MAR00-107 from the Prinses Beatrix Fonds, the Netherlands, and research grant (97252) from the Faculty of Medicine, University of Nijmegen, the Netherlands.

References

Chen DH, Brkanac Z, Verlinde CL, Tan XJ, Bylenok L, Nochlin D, et al. Missense mutations in the regulatory domain of PKC gamma: a new mechanism for dominant nonepisodic cerebellar ataxia. Am J Hum Genet 2003; 72: 839–49.

David G, Giunti P, Abbas N, Coullin P, Stevanin G, Horta W, et al. The gene for autosomal dominant cerebellar ataxia type II is located in a 5-cM region in 3p12-p13: genetic and physical mapping of the SCA7 locus. Am J Hum Genet 1996; 59: 1328–36.

Devos D, Schraen-Maschke S, Vuillaume I, Dujardin K, Naze P, Willoteaux C, et al. Clinical features and genetic analysis of a new form of spinocerebellar ataxia. Neurology 2001; 56: 234–8.

Durr A, Stevanin G, Cancel G, Duyckaerts C, Abbas N, Didierjean O, et al. Spinocerebellar ataxia 3 and Machado-Joseph disease: clinical, molecular, and neuropathological features. Ann Neurol 1996; 39: 490–9.

Flanigan K, Gardner K, Alderson K, Galster B, Otterud B, Leppert MF, et al. Autosomal dominant spinocerebellar ataxia with sensory axonal neuropathy (SCA4): clinical description and genetic localization to chromosome 16q22.1. Am J Hum Genet 1996; 59: 392–9.

Harding AE. Classification of the hereditary ataxias and paraplegias. Lancet 1983; 1: 1151–1155.

Herman-Bert A, Stevanin G, Netter JC, Rascol O, Brassat D, Calvas P, et al. Mapping of spinocerebellar ataxia 13 to chromosome 19q13.3-q13.4 in a family with autosomal dominant cerebellar ataxia and mental retardation. Am J Hum Genet 2000; 67: 229–35.

Holmes SE, O'Hearn EE, McInnis MG, Gorelick-Feldman DA, Kleiderlein JJ, Callahan C, et al. Expansion of a novel CAG trinucleotide repeat in the 5′ region of PPP2R2B is associated with SCA12. Nat Genet 1999; 23: 391–2.

Imbert G, Saudou F, Yvert G, Devys D, Trottier Y, Garnier JM, et al. Cloning of the gene for spinocerebellar ataxia 2 reveals a locus with high sensitivity to expanded CAG/glutamine repeats. Nat Genet 1996; 14: 285–91.

Kawaguchi Y, Okamoto T, Taniwaki M, Aizawa M, Inoue M, Katayama S, et al. CAG expansions in a novel gene for Machado-Joseph disease at chromosome 14q32.1. Nat Genet 1994; 8: 221–8.

Kettner M, Willwohl D, Hubbard GB, Rub U, Dick EJ Jr, Cox AB, et al. Intranuclear aggregation of nonexpanded ataxin-3 in marinesco bodies of the nonhuman primate substantia nigra. Exp Neurol 2002; 176: 117–21.

Knight MA, Kennerson ML, Anney RJ, Matsuura T, Nicholson GA, Salimi-Tari P, et al. Spinocerebellar ataxia type 15 (sca15) maps to 3p24.2–3pter: exclusion of the ITPR1 gene, the human orthologue of an ataxic mouse mutant. Neurobiol Dis 2003; 13: 147–57.

Knight MA, Gardner RJ, Bahlo M, Matsuura T, Dixon JA, Forrest SM, et al. Dominantly inherited ataxia and dysphonia with dentate calcification: spinocerebellar ataxia type 20. Brain 2004; 127: 1172–81.

Koide R, Kobayashi S, Shimohata T, Ikeuchi T, Maruyama M, Saito M, et al. A neurological disease caused by an expanded CAG trinucleotide repeat in

the TATA-binding protein gene: a new polyglutamine disease? Hum Mol Genet 1999; 8: 2047–53.

Koob MD, Moseley ML, Schut LJ, Benzow KA, Bird TD, Day JW, et al. An untranslated CTG expansion causes a novel form of spinocerebellar ataxia (SCA8). Nat Genet 1999; 21: 379–84.

Kumada S, Uchihara T, Hayashi M, Nakamura A, Kikuchi E, Mizutani T, et al. Promyelocytic leukemia protein is redistributed during the formation of intranuclear inclusions independent of polyglutamine expansion: an immunohistochemical study on Marinesco bodies. J Neuropathol Exp Neurol 2002; 61: 984–91.

Lathrop GM, Lalouel JM. Easy calculations of lod scores and genetic risks on small computers. Am J Hum Genet 1984; 36: 460–5.

Matsuura T, Achari M, Khajavi M, Bachinski LL, Zoghbi HY, Ashizawa T. Mapping of the gene for a novel spinocerebellar ataxia with pure cerebellar signs and epilepsy. Ann Neurol 1999; 45: 407–11.

Matsuura T, Yamagata T, Burgess DL, Rasmussen A, Grewal RP, Watase K, et al. Large expansion of the ATTCT pentanucleotide repeat in spinocerebellar ataxia type 10. Nat Genet 2000; 26: 191–4.

Miyoshi Y, Yamada T, Tanimura M, Taniwaki T, Arakawa K, Ohyagi Y, et al. A novel autosomal dominant spinocerebellar ataxia (SCA16) linked to chromosome 8q22.1–24.1. Neurology 2001; 57: 96–100.

Nakamura K, Jeong SY, Uchihara T, Anno M, Nagashima K, Nagashima T, et al. SCA17, a novel autosomal dominant cerebellar ataxia caused by an expanded polyglutamine in TATA-binding protein. Hum Mol Genet 2001; 10: 1441–8.

Orozco G, Estrada R, Perry TL, Arana J, Fernandez R, Gonzalez-Quevedo A, et al. Dominantly inherited olivopontocerebellar atrophy from eastern Cuba. Clinical, neuropathological, and biochemical findings. J Neurol Sci 1989; 93: 37–50.

Orr HT, Chung MY, Banfi S, Kwiatkowski TJ Jr, Servadio A, Beaudet al, et al. Expansion of an unstable trinucleotide CAG repeat in spinocerebellar ataxia type 1. Nat Genet 1993; 4: 221–6.

Paulson HL, Perez MK, Trottier Y, Trojanowski JQ, Subramony SH, Das SS, et al. Intranuclear inclusions of expanded polyglutamine protein in spinocerebellar ataxia type 3. Neuron 1997; 19: 333–44.

Pulst SM, Nechiporuk A, Nechiporuk T, Gispert S, Chen XN, Lopes-Cendes I, et al. Moderate expansion of a normally biallelic trinucleotide repeat in spinocerebellar ataxia type 2. Nat Genet 1996; 14: 269–76.

Ranum LP, Schut LJ, Lundgren JK, Orr HT, Livingston DM. Spinocerebellar ataxia type 5 in a family descended from the grandparents of President Lincoln maps to chromosome 11. Nat Genet 1994; 8: 280–4.

Robitaille Y, Lopes-Cendes I, Becher M, Rouleau G, Clark AW. The neuropathology of CAG repeat diseases: review and update of genetic and molecular features. Brain Pathol 1997; 7: 901–26.

Sanpei K, Takano H, Igarashi S, Sato T, Oyake M, Sasaki H, et al. Identification of the spinocerebellar ataxia type 2 gene using a direct identification of repeat expansion and cloning technique, DIRECT. Nat Genet 1996; 14: 277–84.

Schols L, Bauer P, Schmidt T, Schulte T, Riess O. Autosomal dominant cerebellar ataxias: clinical features, genetics, and pathogenesis. Lancet Neurol 2004; 3: 291–304.

Stevanin G, Bouslam N, Thobois S, Azzedine H, Ravaux L, Boland A, et al. Spinocerebellar ataxia with sensory neuropathy (SCA25) maps to chromosome 2p. Ann Neurol 2004; 55: 97–104.

Swartz BE, Burmeister M, Somers JT, Rottach KG, Bespalova IN, Leigh RJ. A form of inherited cerebellar ataxia with saccadic intrusions, increased saccadic speed, sensory neuropathy, and myoclonus. Ann N Y Acad Sci 2002; 956: 441–4.

van de Warrenburg BP, Sinke RJ, Verschuuren-Bemelmans CC, Scheffer H, Brunt ER, Ippel PF, et al. Spinocerebellar ataxias in the Netherlands: prevalence and age at onset variance analysis. Neurology 2002; 58: 702–8.

van de Warrenburg BP, Verbeek DS, Piersma SJ, Hennekam FA, Pearson PL, Knoers NV, et al. Identification of a novel SCA14 mutation in a Dutch autosomal dominant cerebellar ataxia family. Neurology 2003; 61: 1760–5.

van Swieten JC, Brusse E, de Graaf BM, Krieger E, van de Graaf R, de Koning I, et al. A mutation in the fibroblast growth factor 14 gene is associated with autosomal dominant cerebellar ataxia. Am J Hum Genet 2003; 72: 191–9.

Verbeek DS, Schelhaas JH, Ippel EF, Beemer FA, Pearson PL, Sinke RJ. Identification of a novel SCA locus (SCA19) in a Dutch autosomal dominant cerebellar ataxia family on chromosome region 1p21-q21. Hum Genet 2002; 111: 388–93.

Worth PF, Giunti P, Gardner-Thorpe C, Dixon PH, Davis MB, Wood NW. Autosomal dominant cerebellar ataxia type III: linkage in a large British family to a 7.6-cM region on chromosome 15q14-21.3. Am J Hum Genet 1999; 65: 420–6.

Yabe I, Sasaki H, Chen DH, Raskind WH, Bird TD, Yamashita I, et al. Spinocerebellar ataxia type 14 caused by a mutation in protein kinase C gamma. Arch Neurol 2003; 60: 1749–51.

Yamashita I, Sasaki H, Yabe I, Fukazawa T, Nogoshi S, Komeichi K, et al. A novel locus for dominant cerebellar ataxia (SCA14) maps to a 10.2-cM interval flanked by D19S206 and D19S605 on chromosome 19q13.4-qter. Ann Neurol 2000; 48: 156–63.

Yue Q, Jen JC, Nelson SF, Baloh RW. Progressive ataxia due to a missense mutation in a calcium-channel gene. Am J Hum Genet 1997; 61: 1078–87.

Zhuchenko O, Bailey J, Bonnen P, Ashizawa T, Stockton DW, Amos C, et al. Autosomal dominant cerebellar ataxia (SCA6) associated with small polyglutamine expansions in the alpha 1A-voltage-dependent calcium channel. Nat Genet 1997; 15: 62–9.

Zu L, Figueroa KP, Grewal R, Pulst SM. Mapping of a new autosomal dominant spinocerebellar ataxia to chromosome 22. Am J Hum Genet 1999; 64: 594–9.